HHS Public Access

Author manuscript

Supercond Sci Technol. Author manuscript; available in PMC 2018 January 01.

Published in final edited form as:

Supercond Sci Technol. 2017 January ; 30(1): 014007–. doi:10.1088/0953-2048/30/1/014007.

Conductors for commercial MRI magnets beyond NbTi: requirements and challenges

Michael Parizh[1], **Yuri Lvovsky**[2,4], and **Michael Sumption**[3]

[1]General Electric Global Research

[2]General Electric Healthcare

[3]Materials Science Department, The Ohio State University

Abstract

Magnetic Resonance Imaging (MRI), a powerful medical diagnostic tool, is the largest commercial application of superconductivity. The superconducting magnet is the largest and most expensive component of an MRI system. The magnet configuration is determined by competing requirements including optimized functional performance, patient comfort, ease of siting in a hospital environment, minimum acquisition and lifecycle cost including service. In this paper, we analyze conductor requirements for commercial MRI magnets beyond traditional NbTi conductors, while avoiding links to a particular magnet configuration or design decisions. Potential conductor candidates include MgB_2, ReBCO and BSCCO options. The analysis shows that no MRI-ready non-NbTi conductor is commercially available at the moment. For some conductors, MRI specifications will be difficult to achieve in principle. For others, cost is a key barrier. In some cases, the prospects for developing an MRI-ready conductor are more favorable, but significant developments are still needed. The key needs include the development of, or significant improvements in: (a) conductors specifically designed for MRI applications, with form-fit-and-function readily integratable into the present MRI magnet technology with minimum modifications. Preferably, similar conductors should be available from multiple vendors; (b) conductors with improved quench characteristics, i.e. the ability to carry significant current without damage while in the resistive state; (c) insulation which is compatible with manufacturing and refrigeration technologies; (d) dramatic increases in production and long-length quality control, including large-volume conductor manufacturing technology. In-situ MgB_2 is, perhaps, the closest to meeting commercial and technical requirements to become suitable for commercial MRI.

Conductor technology is an important, but not the only, issue in introduction of HTS / MgB_2 conductor into commercial MRI magnets. These new conductors, even when they meet the above requirements, will likely require numerous modifications and developments in the associated magnet technology.

corresponding author parizh@ge.com.

[4]Current address: Superconducting Design Solutions, SC, USA; yuri.lvovsky@gmail.com

1. Introduction

Magnetic Resonance Imaging (MRI) is one of the primary tools in medical diagnostics [1]. MRI is the only chemically sensitive in-vivo imaging technique with high-resolution soft-tissue contrast. It allows physicians to produce clinically relevant images of soft tissue lesions and functional parameters of body organs, without the use of invasive procedures or ionizing radiation such as X-rays.

Close to 50,000 MRI scanners are installed worldwide. Over 35,000 of these scanners use superconducting magnets. Approximately 4,000 scanners are installed annually including more than 3,000 superconducting systems. An estimated 33.8 million MR procedures were performed in the United States in 2013 vs. 9.1 million in 1995. In the United States in 2013, there were almost 8,000 hospital and non-hospital MRI locations that in total used over 11,000 scanners [2].

Advantages of superconducting MRI systems include better performance, the highest temporal and spatial homogeneity of the magnetic field, high signal-to-noise ratio (SNR), the shortest scan time, and the highest patient throughput. Superconducting scanners are the only configuration for thin slices and high-end applications. Superconducting magnets offer the lowest weight: less than 10 tons for 3 T units. Typical commercial actively-shielded superconducting scanners have no excessive stray magnetic field outside the scan suite.

The overwhelming majority of commercial whole-body superconducting scanners are either 1.5 T or 3 T units. Over 70% of the installed and new superconducting scanners are 1.5 T units. The 1.5 T systems are a good compromise between performance, patient comfort, ease of siting in a hospital environment, optimized installation, and life-cycle cost. Since approximately 2010, the 3 T scanners represent over 20% of the new installations [2]. The 3 T scanners, however, do not represent the fastest-growing MRI segment as they were 5–10 years ago.

The majority of the newly-installed superconducting whole-body scanners are cylindrical in shape. The cylindrical configuration represents the most efficient way to generate a highly uniform magnetic field with the optimal magnet and scanner cost. Cylindrical MRI systems have a known but clinically accepted limitation [3]: a narrow patient bore and >100 cm length. This tunnel creates several issues: (a) obese patients may not fit into the tunnel, (b) a claustrophobic effect causes certain patients to reject the procedure, creating financial loss for the image center and diagnostic loss for the patient, and (c) it restricts interventional medical procedures. To address the narrow-bore issues, a wider, 70-cm patient bore was introduced by Siemens in 2005. Now over half of new MRI installations in developed countries have the wider-bore configuration [2].

Commercial MRI magnets utilize NbTi conductor. The MRI industry uses approximately 4,000 tons of NbTi conductor per year (the weight includes copper stabilizer). The NbTi conductor is a mature, mechanically-strong, manufacturing-friendly material well optimized for MRI production. NbTi magnets are compact, demonstrate reliable performance and are cost-effective. The low critical temperature of 9.3 K is the major disadvantage of NbTi

conductor, which requires operation at liquid helium temperature. This results in a higher refrigeration cost and high on-site construction cost if ventilation ducts need to be built.

The use of NbTi conductor makes MRI the largest user of helium in the world. MRI utilizes about 20% of all helium, compared to only 5% in early 1990s [4], [5]. Cryogenic applications use over 50 million cubic meters of gaseous helium per year (estimated using the data in reference [6]). Consistent increases in helium prices and high helium prices in developing countries affect the growth of the MRI market. Low life-cycle cost, practically quench-free MRI scanners that do not require liquid cryogen may become game changers.

MRI design always involves a compromise, since trade-offs and proven alternative solutions are possible. For a novel solution to be accepted in the marketplace as a game-changer, it must appeal to the clinical users far beyond its pure technical merits, namely by providing unquestionable cost and/or imaging benefits. Therefore, within the trade-offs, MRI designers favor the lowest scanner cost option including the lowest production and life-cycle cost: price of the installed commercial 3T scanner must be below $3M, and even lower for 1.5 T scanners. In most cases, the optimized design decisions lead to the architecture of commercial 1.5 T and 3 T magnets.

This paper analyses alternatives to NbTi conductors for commercial MRI magnets. Potential conductor candidates include MgB_2, ReBCO and BSCCO options. The authors tried to generalize the conductor requirements and avoid links to a particular magnet configuration or design decision.

The eventual market verdict on alternative to NbTi for MRI application depends on many factors. Benefits to the customer (hospitals, physicians and patients) such as improved scanner performance, patient comfort, reduced acquisition and life-cycle cost are the key factors. Cryogenic benefits are among the factors that may favor customer satisfaction. However, in this paper the authors deliberately leave out side-by-side cost comparisons and acceptance predictions, focusing primarily on the analysis of technical requirements and technical readiness of each of the conductor options. Similarly, cryogenic solutions have been given limited consideration here, since the impact of cryogenics on conductor requirements is to some extent limited. Whether it is a helium bath-cooled or “cryogenless” conduction-cooled, besides insignificant differences in available coil envelope and the additional provisions for heat conducting pathways, the key conductor requirements outlined in this paper, such as coil current density, quench protection (assuming present-day-like magnet protection schemes), persistence, conductor quality, winding manufacturability etc. are similar for either cryogenic option. For designs operating above 4K (e.g. for 20K–40K configurations), the conductor parameters such as $\boldsymbol{I_c}$ and $\boldsymbol{N}$-value will be less favorable than the 4K parameters used in this analysis, which will further add to the challenges to fulfill the requirements outlined in this paper.

2. Customer requirements to superconducting MRI scanners and magnets

Cylindrical whole-body scanners represent the mainstream of the clinical MRI imaging. They accommodate the complete human anatomy, as the patient is positioned on the table

and can be advanced along the bore to any position required for the imaging. The imaging takes place in a large, centrally located elliptical or spherical field-of-view (FOV), and the whole-body scanner can cover any part of anatomy of the human body, with the high performance whole-body gradient coils and radio frequency (RF) coil mounted in the magnet bore that ensure high image quality. Such clinical universality, combined with the ever-advancing imaging techniques, has been the key to widespread clinical acceptance of whole-body MRI. In terms of trade-offs, this universality comes at a price of large size, large amount of superconductor and structure and hence of a considerable cost of the whole-body magnet, as well as the amount of helium that is used in traditional cylindrical MRI magnet design.

Specialty MRI scanners, designed for particular aspects (regions) of the human anatomy, present a smaller-sized alternative to the whole-body MRI. Whether it is a head, extremity, or neonate imager, the appeal of a dedicated MRI is rooted in its small envelope and field-of-view, with geometry tailored to the targeted anatomy only. This can potentially deliver lower cost, greater ability to site the scanner within a small specialized room, faster installation, simpler maintenance and more advanced cryogenics [7]. On the flip side, the specialty scanners have obvious drawbacks compared with their whole-body counterparts. The lack of clinical universality is one of the major disadvantages which does not allow to address variation in the scanning needs, or different patient flows in clinical environment, while still requiring construction of an RF-screened imaging room together with the full range of electronic components (albeit of smaller ratings and size). The above drawbacks are responsible for the limited clinical success of specialty scanners so far. Their present market share is limited to less than 5% of the total MRI market.

2.1 Commercial whole-body MRI magnets

Designers of MRI scanners and superconducting magnets must address multiple trade-offs [3], [7]. The high image quality and fast patient throughput require a higher field strength of at least 1.5 tesla, high field homogeneity and temporal field stability in a large volume. High-strength gradient coils are necessary to improve the image quality and reduce the scanning time. Modern gradient coils require additional space for efficient and expensive cooling arrangements, which competes with the magnet design space in the bore. Customers want a low-cost scanner including installation and life-time cost. These requirements may be translated to light weight, compact magnets with reduced stray magnetic field, and low operational cost with minimized or no low helium loss, long helium refill intervals, and low power consumption. Fast installation with minimum on-site construction, minimized maintenance, service at field help in reduction of the life cycle cost of the scanner. Patient comfort is improved in wider-bore, shorter scanners. The latter advantage, however, incurs additional penalty in magnet cost and design risk compared to their longer, narrow bore counterparts.

These conflicting requirements to scanners result in the following top-level Specifications for whole-body MRI magnets:

2.2 Specialty magnets

From purely technical standpoint, specialty MRI magnets have several advantages:

a. Anatomy-targeted geometry often opens up additional optimization options (such as, for example, asymmetric designs [8], [9]). This can lead to non-traditional coil topology, as well as alternative structural and cryogenic solutions. Because of the small dimensions and limited FOV in the specialty scanners, the amount of shimming steel is reduced;

b. The small diameter of the field generating coils translates to a significantly reduced dipole moment and stray field. This allows the forsaking of active shielding coils, which are commonplace in the whole body 1.5T clinical scanners. The absence of shielding coils in the high-temperature superconductor (HTS) specialty magnets not only saves almost half of HTS vs. the shielded design [10]; it also eliminates challenge of high hoop stresses in the shielding coils while drastically simplifying structure and cooling arrangements. For the above reasons all HTS MRI demonstrator designs until now have no shielding coils. While the iron shield they employ may provide sufficient stray field control in a 1.5T specialty magnet, this approach is not feasible for the whole body, or 3T specialty MRI scanners, which require a separate development;

c. Another benefit of the small size of specialty HTS scanners is low stored energy E_{magnet} which involves less support structure. It also makes much easier to protect the magnet during quench, as smaller energy per unit volume is deposited in quench. Smaller coils mean faster normal zone spreading, reduced voltages and peak temperatures;

d. Cryogenics options are also improved. Small dimensions lend themselves better to pure conduction-cooled design, due to shorter, simpler conduction pathways and lesser temperature gradients, especially with absent shield coils. In designs where cryogens are used (either in open bath or closed volume), less volume is required to cool down smaller cold mass.

Table 2 presents comparative examples with parameters for three specialty HTS MRI demonstrators. Obviously, all these proof-of-principle magnets are well below the minimum performance requirements for commercial whole-body MRI scanners outlined in Table 1. Larger warm bore, actively-shielded configuration, improved uniformity and drift will all dramatically increase technical challenges and require significant developments.

Because of the above benefits, the specialty MRI magnets might represent a naturally attractive introductory path for MgB_2 and HTS, as outlined in [7], [14], [15] and illustrated by the examples in Table 2. However, in order to have eventual success in the clinical marketplace, the HTS design must address issues of the wide bore magnet technology. It is due to this consideration and due to the small portion of clinical market currently represented by low-temperature superconductor (LTS) specialty magnets, we will focus this paper on the whole body magnets.

Below we will discuss conductor requirements which are stemming from the needs of commercial whole-body MRI magnets.

3. Design of whole-body MRI magnets

In this section, the major mechanical and electromagnetic characteristics of whole-body MRI magnets will be illustrated in terms of 1.5 tesla scanners. The 1.5 tesla whole-body scanners represent roughly 75% of all superconducting scanners produced in recent years. Magnetic fields in coils, forces, stresses, and energy in the 3 tesla whole-body magnets will be significantly higher. The force as well as the stored energy is roughly proportional to the square of center field while the peak magnetic field in coils and the stresses depend on the particular design.

A multi-coil configuration is typical for magnets up to 4 tesla [7]. As a first approximation, the number and position of coils in multi-coil design, as well as the total amount of conductor can be determined using parametric relations derived in [10] in function of coil envelope and field-of-view. The analysis below allows us to delineate and compare requirements for wide bore MRI magnets with different options.

Parametric analysis was carried out for the typical uniformity of MRI magnets of 10 ppm in 45 cm DSV (diameter spherical volume). The 5 gauss field is located 4 m axially and 2.5 m radially from the iso-center of the magnet. Two options of the coil inner diameters (ID) are evaluated: 90 cm and 100 cm. The former option can be considered as a reference point for the whole-body magnet designs with 60 cm patient bore, while the scanners with the larger 70-cm patient bore are illustrated by superconducting coil ID of 100 cm. We consider magnets with average current densities over the coil winding of 100 Amp/mm^2 and 150 Amp/mm^2. Although superconducting magnets with such parameters do not represent any particular commercial configuration, the analysis is helpful for understanding of the trends and trade-offs.

In order to deliver the required uniformity, actively-shielded superconducting MRI magnets must have at least 8 coils (Figure 1). Ultra-short magnets may require more than eight coils. MRI magnets consist of a set of so called Main coils, six symmetric coils in a typical eight-coil configuration. Two Shielding coils reduce stray magnetic field to a specified level; the current direction in the Shielding coils is opposite to that in the Main coils. The Main coil 1 usually experiences the highest peak field, forces and stresses as compared with other coils. Shielding coils often have the highest magnetic hoop stress.

Electromagnetic analysis demonstrates that the peak magnetic field on conductor in a 1.5T magnet is above 3 tesla, both parallel and perpendicular to the main magnet axis. In shorter magnets, the peak field may increase to 4.5 tesla or even higher. Figure 2 shows that the coil height, and, hence, the peak magnetic field (Figure 3), increases significantly when magnets become shorter. Reduction of the current density has little effect on the coil width and location while the coil height is in reversely proportional to the current density. If the magnets are shorter than about 130 cm for the required uniformity and stray field, the coil height and magnetic field grow fast, typically more than 0.1 tesla of the field increase per 1

cm reduction of the magnet length. Even in longer magnets with reduced bore diameter, the peak field is above 2.5 tesla unless a coil geometry is chosen that significantly extends (spreads) its axial dimension, and the design moving closer toward compensated solenoids used in UHF magnets. For long magnets, reduction of the current density from 150 Amp/mm^2 to 100 Amp/mm^2 helps in the field reduction by about 0.25 tesla.

Conductor in MRI magnets operates at high compressive and tensile stresses. Typical tensile stresses–such as hoop stress - are 50 to 100 MPa. Compression stresses of 20 MPa are not unusual. The coils may experience even higher local stresses. The hoop stress is roughly proportional to current density $\boldsymbol{J_{avg}}$. If not constrained by an external support, the hoop stress in the shielding coils may be a factor of two higher than in the Main coils. Reduction of the bore size has relatively small effect on the hoop stress in the Main coils while it allows a significant reduction of the stress in the Shielding coils adding challenges to design of the actively-shielded magnets. Note that there are design approaches that minimize or even eliminate the tensile stresses during magnet operation. Still, the tensile stress in conductor is unavoidable during coil manufacturing.

Figure 4 shows conductor length necessary to build the magnet, and conductor needs for the larger Main coil #1 and Shielding coil. Note that conductor for shorter coils require more superconducting material (larger superconducting cross-section) due to higher field on conductor. Conductor weight is estimated in assumption of a copper stabilized conductor. The conductor length requirements will be discussed in detail in section 4.7.

The whole-body MRI magnets store a rather high energy of 2 MJ minimum (Figure 5). For a given uniformity, the energy is approximately proportional to cube of the coil bore while the magnet length and current density have little effect. Efficient configurations have high heat loads of 5 to 10 J/gm where the heat load here is defined as a ratio of stored energy to conductor mass. For magnets operating at 20K or lower temperature, such heat loads correspond to an average quench temperature in the magnet of 80K to 90K. Unless properly protected, the magnets may be damaged during quench. All coils must be fully resistive within few seconds after initiation of quench, see the detailed analysis in section 4.3. Efficient quench protection is one of the most challenging requirements to the whole-body MRI magnets made of MgB_2 or HTS.

The parametric analysis above assumes the most cost-effective MRI configurations, with a number of rectangular cross-section superconducting coils, Figure 1. Within each coil we assume a uniform distribution of current. This means that the distance between current-carrying elements (superconducting filaments or tape) is small compared to the coil size. Although typical for commercial MRI magnets, this configuration is not the only option. Conductor length constraints, challenges in force transfer, limitations on the peak field or quench voltages may force the magnet designers to consider other configuration options. For example, the 11.7 tesla Iseult magnet [16] uses 170 double-pancakes (DP) in the main coils. Separation between the DP coils varies to provide the highest uniformity. Other very-high field magnets, 7 tesla and higher, often utilize very long main solenoids and a number of compensation coils. Specialty magnets may use cold or warm iron to minimize the amount of conductor, as seen in Paramed's 0.5T MgB_2 OpenSky scanner [17] that uses the DP coil

configuration as well. While addressing certain technical challenges, these options result in either higher cost, or reduced performance (such as reduced field-of–view).

4. Conductor requirements, challenges and opportunities

In this section, we will derive conductor requirements from the magnet constraints. Certain descriptions and requirements are to a large extent rooted in the traditional, mature, NbTi-based multi-coil magnet configuration that was optimized for commercial whole body MRI magnets. Such design solutions can naturally serve as a starting point and a basis for any benchmarking. Below we will also discuss alternative magnet design and conductor options.

The HTS and MgB_2 conductor technologies offer new opportunities and also introduce new constraints. These opportunities and constraints may offer additional options to be considered for non-traditional approaches presently not used in commercial NbTi magnets. However, for an alternative HTS / MgB_2 (non-NbTi) magnet configuration to succeed in the very competitive commercial marketplace, its merits and trade-offs must compare favorably with the existing, proven, cost-effective and well-established solutions. Obviously, conductor development and development of the magnet technology for a new conductor type should go side-by-side. Differences in solutions for various design areas between NbTi and MgB_2 / HTS-based MRI magnets are illustrated in Table 3 and will be discussed below.

4.1 Magnet uniformity

In order to provide high-quality images, MRI magnets must generate magnetic fields with very high temporal and spatial uniformity on the order of several parts-per-million (ppm) over the whole imaging volume. In typical commercial 1.5 T and 3 T magnets, the field uniformity is on the order of 10 ppm peak-to-peak in about 45 cm diameter volume, Table 1.

MRI system designers may trade off a reduced image volume and system compactness either at a penalty of longer scanning time that assumes, for example, multiple scans to achieve complete extended coverage, or limit system application to dedicated examinations such as brain scanning. The reduced imaging volume, however, has typically a minor effect on conductor requirements including peak field, critical current and conductor length, when compared for a fixed coil envelope. The multi-coil configuration (Figure 1) is the most cost-effective option for compact, high-uniformity scanners. Disadvantages of this option may include higher peak field, high compression stresses and tight positional tolerances.

Positional tolerance is one of the major manufacturing challenges. All coils need to be wound within a pre-manufactured pocket - whether such pocket is an integral part of the former, or used as an off-line tool - with a precise number of turns. Typically, the accumulated misplacement of a turn in the coil pocket needs to be half-a-turn width or less. This means that tolerances on conductor dimensions should be on the order of ±10 micron. The current needs to be evenly and predictably distributed within conductor. The current distribution should not change over time: the latter might be influenced by external effects such as shimming, a change in the background magnetic field caused by moving objects, or the effect of gradient coils. The above requirements mean that a conductor with twisted filaments is a preferred option for MRI.

The presence of magnetic materials in conductor is undesirable. The magnetic materials may result in high local stresses in conductor, they cause degraded, unpredictable uniformity and magnetic field drift.

One issue of HTS MRI that is absent in traditional LTS magnets, is screening currents which are induced in wide superconducting tapes during ramp. It is known that the screening currents in NMR with inserts made of HTS tape may significantly degrade NMR performance [18], [19].

The long decay time of the screening currents means that an installed MRI magnet would require periodic post-installation re-shimming when the harmonics from decaying currents start to diminish. The issue may be handled, for example, by providing sufficient capacity of shimming coils embedded into the gradient coils, which obviously impacts complexity and cost of the scanner as they need shimming to be adjusted as the screening currents decay.

4.2 Persistence

The typical guaranteed long-time field decay in MRI magnets needs to be less than 0.1 ppm/hour. This means that the center field will not degrade by more than 0.088% per year. Higher field decay will result in frequent needs to re-ramp the magnet which will incur higher operating cost in a commercial environment.

The total voltage across the magnet U and the total resistance of the circuit R_c may be estimated as:

$$U < 2\,decay \times E_{magnet}/(3600 \times I_o), \quad R_c < 2\,decay \times E_{magnet}/(3600 \times I_o{}^2) \quad (1)$$

where ***decay*** is the field decay (in ppm per hour), E_{magnet} is the magnet energy (in mega-joules) and I_o is the magnet current (in Amps). For a whole-body 1.5 T scanner, E_{magnet} is on the order 2 to 3 MJ (Figure 5). Assuming an operating current of 500 Amp, the total voltage drop across the magnet will be less than 0.3 micro-volt, and the total circuit resistance will be below 0.5 nano-ohm.

There are leading two mechanisms of long-term field decay in persistent magnets:

1. Field decay due to resistance of joints;
2. Field decay in the conductor due to non-sharp transition from superconducting to the resistive state.

From the estimate above, the resistance of individual joints must be less than 10^{-11} ohm. Joints in MRI magnets are typically expected to operate in a background field of up to 0.5 tesla in 1.5 T magnets, and up to 1 tesla in 3 T scanners. Shielding of the joints, although feasible, increases the magnet cost.

The voltage drop across conductor may be expressed as

$$V/V_c=(I/I_c)^N, \quad (2)$$

where V is the voltage drop across a sample, V_c is the voltage criterion (typically, 1 micro-volt/cm), I is current and I_c is the critical current at given field and temperature, index N is the best-fit value for the current-voltage curve.

The index N (or N-value) depends on superconducting materials. While the N-value is ultimately limited by the depth of the individual fluxon pins (related to flux creep) in otherwise perfect materials, extrinsic limits like filament sausaging may also play a role. [20]. For NbTi the index N is typically above 40 at background fields below 7 tesla. In HTS materials, especially when operated at higher temperatures, the relative pinning strength is comparatively lower as compared to the thermal activation, which leads to flux creep, but extrinsic limitations on N may be just as important ([21] and references there), especially at low temperatures. The N-value in HTS conductor is often below 30 and in some cases degrades to less than 20 at a relatively low background field of 0.5 tesla. The N-values in HTS vary dramatically not only due to physical factors such as field, temperature and orientation but from vendor to vendor even for similar conductor types.

From Eq. (2), reduction of the guaranteed N-value by a factor of two requires operation at a current $I/\sqrt{2}$, or about 30% lower to achieve the same low voltage drop (or the magnet field decay). Due to significant variability of the field across the coils, it is difficult to estimate the effect of N-value on the voltage drop in the actual magnets. The curves are not universal and should be calculated for each particular magnet and conductor configuration. For conduction-cooled and MgB_2 / HTS magnets, additional factors must be considered such as possible temperature variability. Because most of the decay occurs in small areas with the highest field, only guaranteed N-values should be used. Figure 6 illustrates a reduction of the operating current needed to ensure a specified field decay for a particular magnet configuration. If the N-value is 30, this magnet can operate at 65% of I_c. If the N-value is 15, the magnet must operate at no more than 40% of the critical current in order to meet the field decay requirements.

As an alternative to relying on future success in HTS joint development, resistive joints used in conjunction with a highly stabilized current supply may be an option. The introduction of embedded leads for external quench dump goes hand in hand with this approach. This approach is presently avoided in commercial LTS MRI magnets. The high-stability supplies are expensive. Although adequate for some routine MRI applications, the field stability in driven magnets is inferior to persistent magnets. In addition, the loss in high-current leads will put additional load on the cryogenic system, especially in cryogen-less configurations. Use of filtering components, e.g. like that used by the 11.7 tesla Iseult circuit [22] may help alleviate cost increase from the high quality power supply.

4.3 Stability and quench protection

Conductor stability is one of the key drivers in the LTS magnet design, forcing solutions that limit potential frictional movements at conductor and coil interfaces to a several-micron

level. Dramatically increased enthalpy and temperature margins in HTS / MgB_2 conductor results in the increase of the minimum quench energy by several orders of magnitude. Therefore, the conductor micro-motion or other small-scale mechanical effects should not cause accidental quenches of the HTS / MgB_2 magnets. In the indirectly-cooled magnet configurations, different stability-related issues come forward, such as control of external heat input sources from leads and switches, or losses due to low-level index ***N***. However, limits on winding tightness and positional tolerances must still be imposed by perhaps more relaxed but no less important factors: a) shimmability; b) efficient through-the-coil conduction in cryogen-free magnets; c) displacements control in HTS conductors - stress sensitivity of oxide conductor requires special control of stresses, including axial and hoop stress in pancakes. Together with the different coil topology options, change in requirements on positional displacements may enable structural options not employed in LTS MRI magnets.

Although HTS / MgB_2 conductors are stable and should not quench without significant external influence, there is always a possibility of unfortunate events that may cause the magnet to quench. These include, for example, failure of the cryogenic system, local overheating due to interaction of the scanner components, personnel errors or hardware malfunctions.

In addition, patient / personnel safety requires a possibility for fast shut down of the magnet within typically less than 30 seconds [23]. A forced magnet quench is a typical method for the fast ramp down, with all or most stored energy released within the cryostat. Present clinical MRI magnets rely on a passive quench detection/protection system that spreads the energy by initiating secondary normal zones in multiple coils.

Obviously, the magnet must not be damaged or show performance degradation in case of quench. Even a remote possibility of magnet damage at a hospital installation is unacceptable for commercial scanners. The properties of HTS / MgB_2 conductors, while including improved stability, have other aspects that create challenges for the quench protection of the MRI magnets, especially for efficient commercial configurations with stored energy above 0.5 MJ and the average current density above 100 A/mm^2. Slow normal zone propagation[3] increases the quench detection time and the protection activation time which poses a danger of local overheating at the quench origin, before the quench protection system can have the opportunity to react.

Let us use the adiabatic MIIT criterion to estimate the maximum protection time in the magnets with passive protection, i.e. the time necessary to reduce current to zero or a close value:

$$\int_{T_o}^{T_{max}} \frac{C\,dT}{\rho} = \int_0^{t_o} J^2 dt, \quad (3)$$

[3]The normal zone propagation velocity in adiabatic conditions $\boldsymbol{V_{nz} \sim J_{avg}/(C\cdot\Delta T^{1/2})\cdot(\rho\cdot k)^{1/2}}$ where $\boldsymbol{\Delta T = T_c - T_{op}}$, $\boldsymbol{T_{op}}$ is the magnet operating temperature, $\boldsymbol{k}$ is thermal conductivity. $\boldsymbol{V_{nz}}$ in HTS / MgB_2 is two orders of magnitude or more lower as compared to NbTi due to high specific heat $\boldsymbol{C}$ at higher operating temperature and high $\boldsymbol{T_c}$.

Here C and ρ are the specific heat and resistivity of the conductor, T_o and T_{max} are initial and the maximum acceptable conductor temperature at the hot-spot location, J is the current density distributed evenly in the conductor cross-section, and t_o is quench time when current is zero.

The adiabatic MIIT criterion provides a reasonable estimate of the peak temperature in the flat central area of the normal zone profile, where conduction to the adjacent parts of the coil can be neglected, and the joule heat generated in conductors is absorbed by coil enthalpy alone [24]. In (3), we use enthalpy of the bare conductor only, while additional insulating and structural components in certain coil configurations can substantially add to the total heat absorbing capacity. Therefore, our estimates below may represent conservative values.

For simplicity, we assume that current remains constant from time zero to t_o. Then, the right integral in Eq. (3) is equal $J^2 \times t_o$. The available time t_o is driven by low-resistivity stabilizing material in the conductor. Examples of the stabilizer include copper or the use of a sheath material (such as Glidcop) with a higher thermal conductivity and lower electrical resistivity [25]. The values of the left-hand integrals are given in [26] for a variety of materials. For OFHC copper with the residual resistivity ratio (RRR) of 100 and T_{max} equal to the room temperature, the integral is equal to about 1.5×10^{17} sec_Amp^2/m^4. The integral is significantly lower for higher-resistivity materials: the integral is on the order of 10^{15} Amp^2_sec/m^4 for NbTi and materials used in HTS conductors.

Assuming that the low-resistance shunting materials occupy only half of the cross-section, the quench time must be less than

$$t_o < 5 \times 10^{16}\ \mathrm{Amp^2\_sec/m^4}/J^2 \quad (4)$$

Eq. (4) gives the quench time of up to 2.2 sec for J = 150 Amp/mm^2, and 5 sec for J = 100 Amp/mm^2. This timing is consistent with results of the detail quench analysis for MgB_2 coils [27]. The latter reference shows that time to reach the room temperature is on the order of 2–3 seconds at J = 175 Amp/mm^2, and that available quench time is significantly shorter if the fraction of stabilizing material is smaller. The quench time includes quench detection, activation of the protection circuit, propagation of the normal zone through the whole or majority of the coil cross-section, and current decay. For the internal passive protection, the conductor shall be designed to withstand - in adiabatic conditions - the full operating current for about twice the quench time t_o without overheating above 100°C and any performance degradation of either conductor or the coil.

Passive quench protection may not be feasible for the MgB_2 / HTS whole-body magnets. The latter units may require an external energy dump due to inability quickly and effectively spread the secondary zones. With the external dump, embedded leads become a necessity. The magnet design will need to accommodate high voltage on the order of 1 kV driven by fast evacuation of the stored energy over 2 MJ for the 1.5T whole-body magnets. If the magnet is designed to operate in the persistent mode, such high voltage across the leads

creates significant challenge: it requires either very high-resistance, large-volume switch, or ability of the switch to carry significant currents well over 10 Amp while open (in resistive mode). All these features create extra complexity and cost of the clinical system with added external cables and dump resistor components.

The no-insulation approach [28] is successful for quench protection in relatively small HTS magnets with stored energy below 1 MJ. The no-insulation approach, however, may have significant disadvantages if used in commercial MRI magnets. Such magnets may require a very long ramp time and have long settling time. There is a high potential for screening currents to affect uniformity. Interaction with gradient coils may cause uniformity drift or even quench.

4.4 Conductor shape

The use of wider tape -the only viable configuration for ReBCO - instead of the traditional NbTi wire has significant implications in MRI design. It impacts coils topology, support structure and manufacture process. With the layer winding, one would need to overcome challenges of the long conductor lengths, long interlayer transitions and provide extra spaces to accommodate large radii of coil in/out leads while the pancake coils would involve multiple inter-pancake joints at the coil outer diameter (OD). With the pancake approach, one can see a potential of coil topology switching from the traditional 8-coil multi-coil design to multiple pancakes or pancake blocks. In order to deliver required homogeneity, such pancakes/blocks would be strategically distributed axially, spaced apart and separated by spacers that support inter-pancake forces [22], [29].

4.5 Insulation

Conductor insulation is one of the critical issues that drives the design of the magnet. Reliable, high-quality, low-cost insulation must be compatible with the coil winding process and cryogenics. Commercial NbTi wires use two types of insulation: approximately 40-micron thick varnish, typically formvar, and braid. Both varnish and braid are continuously applied to the conductor. Varnish is a mature, cost-efficient, high-strength insulation (BDV over 3 kV [30, part 3]). During varnish application, the wire is heated–although for a short time–to temperature above 400°C. This process must not result in the conductor damage or degradation of superconducting properties. Formvar is a low thermal class material (class 105). This means that any exposure to temperature above 130°C may result in the insulation damage [30, clause 1.8]. Formvar-insulated wire can be used in epoxy-impregnated coils if the epoxy temperature does not exceed 120°C during application and curing. The latter may preclude the use of formvar-insulated conductor in the vacuum-impregnated coils (VPI) that are typically cured at temperature close to 200°C. Low thermal resistance formvar-insulated wire is a preferred material for use in conduction-cooled magnets that do not carry liquid cryogen. However, quality of varnish insulation deposited over conductors with irregular, non-smooth cross-sections (e.g. wire-in-channel (WIC), HTS tapes with sharp corners, etc.) may present significant challenge not faced by monolith round or rectangular conductors.

The wire-in-channel conductor typically uses a polyester braid insulation, about 150-micron thick. The braid is essentially a separator; its breakdown voltage (BDV) is typically less than

1 kV. The braid-insulated conductor can be used in dry- and wet-wound coils, and in VPI coils. The high thermal resistance of the braid is disadvantageous for the cryogen-less magnets, unless the braid is substantially permeated by epoxy with high thermal conductivity.

HTS and MgB_2 conductors often use kapton tape insulation. The tape, although acceptable for relatively small magnets, has relatively low guaranteed breakdown voltage: unavoidable insulation gaps between turns of the tape may result in electrical shorts and even damage of the magnet.

Conductor insulation must be selected to be consistent with the magnet protection. If the conductor is insulated, the insulation must be designed for the inter-layer voltage of several hundred volts. The hot spot temperature during quench may be up to 100°C. This high temperature must not cause any magnet damage or performance degradation.

4.6 Refrigeration

One of key HTS benefits is the potential for different cryogenics that operate more efficiently at higher temperatures. The use of traditional helium bath in commercial MRI with new superconductors would only be accepted if they manage to directly beat NbTi on cost and manufacturability–definitely an uphill battle. Meaningful cooling alternatives include either full “dry” conduction cooling, or low-volume close loop systems that can tolerate T_{op} significantly above the present 4K. The use of different, higher temperature cryogens, such as LH_2 [7] can become a game changer at a later stage of HTS introduction into MRI design. Conduction-cooled magnets have intrinsic issue of ride-through limitation. To resolve it, the design may resort to high-enthalpy thermal batteries–an approach that has been explored in various applications [31], [32], [33], and which could substantially change topological arrangements inside MRI magnet.

4.7 Manufacturability

A low-cost, high yield manufacturing process is paramount for commercial MRI magnets. Any conductor must be consistent with the coil winding technology: dry, wet winding using epoxy, paraffin wax or other compounds, or VPI. For commercial MRI magnets manufacturers, a react and wind approach has significant advantage over the wind and react option: no coil heat treatment after winding. Such heat treatment will significantly increase the production time and limit cost-effective design options. In many cases, it would also limit manufacturing options to the assembly of individually produced off-line and then heat-treated coils, rather than direct winding inside a common former.

To achieve a low price for commercial MRI magnets, manufacturers must assure high yield of the conductor. This requires low conductor breakage rate, minimum scrap, minimum failure in magnets. MRI magnets must meet all requirements: the magnet operation of 1% below the nominal field, or field decay of only 10% above specification are unacceptable.

The 1.5T whole body MRI magnets require 15 to 20 kAmp-km of conductor, with total weight on the order of 500 kg or more (Figure 4a). Assuming operating current of 500 Amp, the magnets need 30 to 40 km of conductor. The larger Main coil #1 (Figure 1) and

Shielding coil require a minimum of 5 km conductor each. In order to minimize the number of joints and reduce cost in the layer-wound coils, no more than two conductor pieces per coil can be used. Therefore, most part of the conductor, say, more than 70%, shall be delivered in lengths in excess of 3 km. The remaining conductor shall have piece lengths 1 km or longer. Reduced piece length will increase scrap and require additional joints. The additional joints will increase the magnet cost and may increase the field decay. Preferably, all conductor should be delivered ready to be wound: no treatment, inspection or testing should be required at the magnet production plants. Conductor vendors must guarantee all properties over 100% of the conductor length including electrical, mechanical, thermal and dimensional specifications. It is highly desirable that the same form-fit-and-function conductor is available from multiple vendors.

4.8 Conductor price

Design of commercial MRI magnets is cost-driven while the magnets and scanners must provide the specified performance. NbTi conductor for MRI is the lowest cost superconducting material, priced at about $1,000 per kAmp-km of the critical current at 4 T, 4.2 K [3]. Figure 4a shows that the total length of conductor for 1.5 T whole-body scanners ranges from about 15 kAmp-km for the smaller bore, longer scanners up to over 20 kAmp-km for the wide-bore, short length scanners. In Figure 4, the operating current is considered rather than the critical current in conductor. Per Figure 6, magnets made of NbTi conductor with high guaranteed ***N***-value of over 35 may operate at 70% of the critical current. Other considerations such as stability, quench protection, cryogenics may lead designers to operation at, say, 50% of the critical current. Therefore, the conductor price for the 1.5 T NbTi scanner may range from about $25k to $50k. Obviously, this is an estimate only. The actual conductor price depends on multiple details that are outside of the scope of this publication. The estimate, however, is a reasonable approximation of the acceptable price of HTS in large volume production.

MgB_2 / HTS conductor promises to simplify cryogenics and reduce life-cycle cost by eliminating the need in helium and other liquid cryogens.

4.9 Conductor Specification for commercial whole-body MRI magnets

Table 4 summarizes requirements for conductors in MRI magnets. The table includes multiple trade-offs. For example, the ***N***-value may be reduced if the critical current and J_{eng} are increased. Higher operating temperature will help to simplify cryogenics while it will cause the increase of the conductor cost. The yield strength may be reduced at the expense of additional structural components. The relaxed dimensional tolerances will require additional shimming capacity that will incur additional cost, occupy expensive space in the magnet bore and may cause uniformity drift. The conductor requirements in this section should be considered as a minimum commercially-competitive specification.

5. Non-NbTi conductor options

In this section, we consider different conductor types to see whether they can meet the requirements listed in Table 4. Table 5 shows a variety of conductors and their level of

compliance with this specification. Analyzing these conductors by this set of requirements is not as straightforward as it might seem at first. In most cases, the available Nb_3Sn, HTS and MgB_2 conductors are not optimized for MRI specifications. For example, MRI magnet designs typically call for a relatively high amount of stabilizer, either in the conductor itself, or added on externally. Commercially available Nb_3Sn conductors are aimed at higher field, more aggressive applications like particle accelerators or research magnets (where occasional quenching is acceptable), or fusion, but in all cases the stabilizer (copper) fraction is intentionally much lower than that needed for MRI applications. In fact, most of the HTS/MgB_2 conductors are designed at much lower stabilizer (copper) fractions than MRI conductors. Beyond this, the conductors overall size and in some cases aspect ratios were not chosen with MRI magnets in mind. So, below we do our best to consider some of these aspects and project accordingly.

We also included Nb_3Sn for comparison among other non-NbTi alternatives. It should be pointed out that Nb_3Sn coils have been considered and are presently used for high field (B_0>7T) NMR magnets, mostly in hybrid designs, in combination with NbTi coils, where the additional margin that Nb_3Sn provides at high fields is essential. However, it is difficult to advocate for use of Nb_3Sn in 1.5T whole-body MRI magnets, with the peak field on conductor below 5 tesla. In this application, the use of Nb_3Sn conductor significantly increases the design and manufacturing complexity and the overall magnet cost. The authors are not aware of any clinical ultra-high field MRI magnets that use Nb_3Sn conductor, although Nb_3Sn could have an advantage here. Similarly, Nb_3Sn conductor might be considered in the case of a conduction cooled system where higher temperature margins are needed. The 0.5 T Magnetic Resonance Therapy (MRT) scanner [34] introduced by General Electric in 1990s is an example of the latter approach. It should be noted, however, that since then the substantial advances in commercial cryocoolers capacity as well as in the magnet design made possible today a whole-body conduction-cooled MRI magnet design with the traditional NbTi conductor.

Of course, there are multiple HTS, MgB_2, and Nb_3Sn sub-strand types and manufacturers, which further complicates the analysis. We have thus chosen a subset of selected (or representative) manufacturers, and described their most relevant conductors.

For MgB_2, HyperTech Research and Columbus Superconductors are well known for manufacturing in-situ [35], [36], and ex-situ MgB_2 [37], [38] respectively. For the HTS conductors, several manufacturers also exist, but the conductors selected are representative. A variety of Nb_3Sn conductors exist, including conductors designed for fusion and high energy physics applications. However, for MRI use, a set of distinct but related conductors designated Nb_3Sn Tube (HyperTech, [39]), and PIT (Bruker [40] and Supramagnetics [41]) are most relevant, and we choose the HTR tube conductor as representative here.

Conductor shape

All conductor types except the coated conductor and Bi:2223 are available as round or rectangular wire. MgB_2 is available as either round or rectangular for either in-situ or ex-situ approaches. Bi:2212 and Nb_3Sn are typically produced round, although there is no apparent

barrier to making them in a rectangular form. Bi:2223 and YBCO coated conductor are made available only as tapes, and are limited to this geometry.

Filament size

The multi-filament conductor is available for all conductor types but ReBCO. MgB_2 conductor can range be readily available at the 40 micron filaments for either the in-situ or ex-situ approach, although typical tape conductors from Columbus have non-round filaments with high aspect ratio [37], [38]. The Bi:2212 and Bi:2223 conductor have relatively larger filaments, for Bi:2212 this is due to filamentary bridging, for Bi:2223 this is due to filamentary aspect ratios. YBCO tapes are at present monolithic, and thus have very wide filament sizes perpendicular to the tape (and very thin parallel to it). The twist pitch values for all conductors are within the requirements of Table 4, except for YBCO which is monolithic.

Critical current $\boldsymbol{I_c}$ per Table 4 should be above 400 A at an operating temperature and 3 T. This is described in Table 4 in terms of the typical conductor size (for application relevant conductors) and the $\boldsymbol{I_c}$ at the specific conditions, and the requirement is met for all conductors except the ex-situ MgB_2. The next criterion is for the critical current in the winding to be above 250 A/mm^2, including the insulation and epoxy, if present. In order to make a fair comparison, we set the J_c reduction (or area reduction) to be 15% of the total for all conductors in order to calculate $J_{e,w}$. This may be most accurate for low aspect ratio rectangular conductors. This requirement was met for all conductors except the ex-situ MgB_2.

The yield strength requirement and piece length requirement were met for all conductors, and the N-value requirement was met for all conductors except Bi:2212 and Bi:2223 conductors. Only the MgB_2 conductors are typically magnetic as now manufactured, although it is known that non-magnetic versions of these conductors are under development. This magnetic response is relatively slight, and comparable to the magnetization from the superconducting filaments themselves.

The requirement for minimum bending radius is < 50 mm. When discussing this requirement, it is important to discuss whether the conductor is to be used in a Wind and React (W&R) or React and Wind (R&W) mode. For YBCO and the ex-situ version of MgB_2, the conductors are only supplied after reaction. On the other hand, YBCO tape has aspect ratio (width : height) and thus has an easy and hard bend direction, the easy direction is listed in Table 5. The minimum bending requirement is met outright only by YBCO and only assuming bending is the easy direction which creates certain limitations in manufacturing options for layer-wound coils. The minimum bending radius for ex-situ MgB_2 is within 20% of this mark, but again, only in the easy bending direction. The in-situ approach for MgB_2 can only meet this requirement is used in a W&R mode. It is worthwhile to mention that this requirement is driven not by the coil size (the bending radius of which all these conductors could meet), but by end-of coil handling (coil leads). If the approach to coil terminations is modified, this constraint could be relaxed, and most of these conductors would meet specification, and all would be usable in R&W mode.

Quench protection

Here we have re-cast this in terms of how many seconds of operation (under full current) the conductor has after a quench initiates before it reaches 100 °C locally. We have used a simple approach [49] to give a first cut answer to this problem, where $Z/J_{eng}^2 = \tau(A_m/A_{cd})$, where A_m is the area of the matrix and A_{cd} is the total cross sectional area of the composite. In case that a significant amount of copper stabilizer is used, $Z = 10^5$ A^2s/mm^4, and from this we can calculate τ. It is in this requirement that most conductor fall short, as fabricated, as can be seen by the values given in Table 5. On the other hand, this should not be a surprise, since the NbTi conductor which is presently being used for MRI has been specifically designed with this parameter in mind. For NbTi conductors, two different approaches are used. Both approaches were proposed by J. Stekly in early1960s and assume the use of significant amount of a low-resistance, high thermal conductivity stabilizing material such as copper or aluminum [50]. In the first approach of the monolith conductor, the NbTi wire itself is designed to incorporate a relatively large amount of copper, enough to increase protection time to the needed level. In the second wire-in-channel (WIC) approach, a NbTi conductor with a relatively low fraction of copper is embedded in a copper channel, and the composite conductor reaches the needed Cu fraction for magnet protection.

Such modifications have not been made to production conductors in Table 5 (except Nb_3Sn). However, the manufacturers should be able to add the needed amount of copper, either by the WIC approach, paralleling that of some NbTi conductors, or by soldering a copper strip onto a rectangular strand (e.g., MgB_2 strand), or by electroplating onto the starting conductor as is typically done for YBCO. In this case, the question then becomes how much is $J_{e,w}$ degraded by this process. We have chosen to approach this by adding enough stabilizer to hit the minimum $J_{e,w}$ target given in Table 4, and then calculate the resulting time for protection, and the value is given in Table 5. Most of the conductors fare well in this process; the one exception is ex-situ MgB_2 (although in-situ MgB_2 fares well).

Persistent joints are routinely available for Nb_3Sn conductor to be used in commercial NMR magnets. There are reports describing successful joints for MgB_2 conductor, for example [51] – [53]: The MgB_2 joints, however, still require significant development to be acceptable for commercial production environment. In particular, the yield of successful joints shall be above 95% minimum. Repeatable and reliable persistent joints for Bi:2212, Bi:2223, or ReBCO conductors had not been developed yet although there are reports describing successful attempts, for example [54].

If we exclude cost from consideration, it would seem that in-situ MgB_2, YBCO, and Nb_3Sn come closest to meeting the needed specifications for a 1.5 T, 4 K MRI. Ex-situ MgB_2 falls short in I_c and J_e, suggesting it is better suited for lower field MRI. Bi:2212 and Bi:2223 fail to meet the N-value specification, although of course they can be used either with active power supplies or by operating at a relatively low fraction of I/I_c–but these are typically undesirable and costly choices. The tube type (and by extension PIT type) Nb_3Sn meets all requirements, except minimum bending radius in R&W mode. Thus it can be used either in the wind-and-react (W&R) mode which incurs an additional magnet manufacturing cost, or used in the react-and-wind (R&W) mode with modifications to the approach to terminations. In situ MgB_2 is in a similar position as Nb_3Sn, meeting all requirements except requiring

either use in W&R mode, or a use I R&W mode with a modification the approach to coil terminations. YBCO meets most requirements, but does have the significant disadvantage of a lack of persistent joint technology.

In the above discussion, we have limited ourselves to the technical aspects of the conductors, but have ignored costs. However, when these considerations are added, it is clear that given that YBCO coated conductors are presently 10–20 times the per meter cost of MgB_2 or Nb_3Sn, these conductors have a significant disadvantage which can only be overcome by a huge reduction in cost for YBCO. This coupled with the lack of persistent joints for YBCO suggests that the conductors which best fit the 4 K, 1.5 T application space (besides NbTi) are in-situ route MgB_2 and powder-in-tube (PIT) or Tube type Nb_3Sn. These conductors bear a more detailed examination against NbTi for this application, where the potential for cost benefits of conduction cooling mode are weighed in.

6. Conclusion

We outlined conductor requirements for commercial whole-body MRI magnets and evaluated possible conductor options. From a technical point of view, none of the HTS or MgB_2 conductor meets the minimum specification for commercial MRI magnets at the moment. For some conductors, MRI specifications will be difficult to achieve in principle. For other, cost is a key barrier. In some cases, the prospects for developing an MRI-ready conductor are more favorable, but developments are still needed.

In the development of MRI-specific designs, quench characteristics, i.e. the conductor ability to carry significant currents without damage while in the resistive state is the common issue that must be addressed. It is shown that any conductor type for use in the whole-body MRI magnets requires a significant amount of a low-resistance stabilizing material such as copper to be added. The stabilizer is likely to occupy at least 50% of the conductor cross-section.

Selection of a proper insulation that is compatible with the coil winding process and cryogenic approach is another challenge. A mature, high-quality, low-cost formvar-type varnish insulation is a preferred insulation, especially in the cryogen-less magnets.

The development of MRI-specific designs and proven long length and quality of the non-NbTi conductor is required before MRI producers will decide to consider alternative materials for commercial MRI scanners. The worldwide production of an alternative conductor should exceed 100 tons a year to be seriously considered as NbTi replacement in commercial MRI magnets. The same form-fit-and-function conductor shall be available from multiple vendors. Conductor manufacturing technologies that guarantee specified properties over 100% conductor length need to be developed.

The in-situ MgB_2 conductor is, perhaps, the closest to commercial MRI requirements. This conductor still needs developments including but not limited to development of an MRI-specific conductor design which is properly stabilized, affordable, and commercially available in long lengths. MRI manufacturers prefer conductor that does not require processing after winding.

Conductor technology is an important but not the only issue in introduction of HTS / MgB_2 conductor in commercial MRI magnets. These new conductors, even when the meet the above requirements, will likely require modifications in the magnet technologies. Efficient technologies shall be developed including efficient winding technologies, reliable passive quench protection with fast detection of the normal zone and prompt current decay, superconducting joints, thermal switches that are compatible with HTS / MgB_2 and can operate at elevated temperature. Refrigeration should be optimized for HTS / MgB_2 conductor: lower operating temperature results in lower conductor cost, while increasing the refrigeration cost.

Finally, the eventual acceptance in the marketplace of the new conductors for MRI magnets will be to large extent determined by the impact that new magnet technology has on the total life cost of new systems for their clinical users. That includes cost of magnet components (superconductor being primary one), cost of manufacture, and cost of service of the installed scanner with the account of impact of its cryogenics.

Acknowledgments

The authors thank E.W. Collings for discussions. Michael Parizh and Yuri Lvovsky are grateful to numerous colleagues in GE Healthcare and GE Global Research for encouragement, support and helpful recommendations. Funding for M.D. Sumption was provided by the National Institute of Biomedical Imaging and Bioengineering, under grant R01EB018363.

References

1. Fritz JV. Neuroimaging Trends and Future Outlook. Neurologic Clinics. 2014; 32:1–29. [PubMed: 24287383]
2. 2013 MR Market Outlook Report. IMV Medical Information Division, Inc; 2013. www.imvinfo.com
3. Cosmus TC, Parizh M. Advances in Whole-Body MRI Magnets. IEEE Transactions on Applied Superconductivity. 2011; 21:2104–2109.
4. Cai, Z., Clarke, RH., Nuttall, WJ. Helium demand: applications, prices and substitution. In: Nuttall, WJ.Clarke, RH., Glowacki, BA., editors. The Future of Helium as a Natural Resource. Routledge; London, UK: 2012.
5. Kornbluth, Ph. Evolution of the global helium business, 1990–2015. CryoGas International. Sep. 2015 :34–36.
6. Glowacki BA, Nuttall WJ, Clarke RH. Beyond the Helium Conundrum. IEEE Transactions on Applied Superconductivity. 2013; 23:0500113.
7. Lvovsky Y, Stautner EW, Zhang T. Novel technologies and configurations of superconducting magnets for MRI. Superconductor Science and Technology. 2013; 26:093001. (71p.).
8. van Oort JM, Laskaris ET, Thompson PS, Dorri B, Herd KG. A cryogen-free 0.5 T MRI magnet for head imaging. Advances in Cryogenic Engineering. 1998; 43:139–47.
9. Sekino M, Ohsaki H, Wada H, Hisatsune T, Ozaki O, Kiyoshi T. Fabrication of an MRI model magnet with an off-centered distribution of homogeneous magnetic field zone. IEEE Transactions on Applied Superconductivity. 2010; 20:781–785.
10. Lvovsky Y. Parametric Relations in Multi-Coil Cylindrical MRI Magnet Design. IEEE Transactions on Applied Superconductivity. 2016; 26(4):4400605.
11. Parkinson B, Slade R, Mallett MD, Chamritski V. Development of a Cryogen Free 1.5 T YBCO HTS Magnet for MRI. IEEE Transactions on Applied Superconductivity. 2013; 23(3):4400405.

12. Terao Y, Ozaki O, Ichihara Ch, Kawashima Sh, Hase T, et al. Newly Designed 3 T MRI Magnet Wound with Bi-2223 Tape Conductors. IEEE Transactions on Applied Superconductivity. 2013; 23(3):4400904.
13. Yokoyama, Sh, Lee, J., Imura, T., Matsuda, T., Inoue, T., et al. Research and Development of the Very Stable Magnetic Field HTS Coil System Fundamental Technology for MRI. 2015 International Symposium on Superconductivity ISS-2015, paper SA-9-INV; 2015; Mitsubishi Corp; May 24. 2016 press-release http://www.mitsubishielectric.com/news/2016/pdf/0524.pdf
14. Xu M, Laskaris ET, Budesheim E, Conte G, Huang X, Stautner W, Amm K. BSCCO MRI Magnet Winding and Testing at LN_2 Temperature. IEEE Transactions on Applied Superconductivity. 2010; 20(3):769–772.
15. Mine S, Xu M, Bai Ye, Buresh S, Stautner W, Immer Ch, Laskaris ET, Amm K. Development of a 3 T–250 mm Bore MgB_2 Magnet System. IEEE Transactions on Applied Superconductivity. 2015; 25(3):4600604.
16. Schild, Th, Aubert, G., Berriaud, C., Bredy, P., Juster, FP., Meuris, C., Nunio, F., Quettier, L., Rey, JM., Vedrine, P. The Iseult/INUMAC whole body 11.7 T MRI magnet design. IEEE Transactions on Applied Superconductivity. 2008; 18:904–907.
17. Paramed website. www.paramedmedicalsystems.com
18. Ahn MC, Yagai T, Hahn S, Ando R, Bascuñán J, Iwasa Y. Spatial and temporal variations of a screening current induced magnetic field in a double-pancake HTS insert of an LTS/HTS NMR Magnet. IEEE Transactions on Applied Superconductivity. 2009; 19(3):2269–2272. [PubMed: 20401187]
19. Maeda H, Yanagisawa Y. Recent Developments in High-Temperature Superconducting Magnet Technology (Review). IEEE Transactions on Applied Superconductivity. 2014; 24(3):4602412.
20. Warnes WH, Larbalestier DC. Analytical technique for deriving the distribution of critical currents in a superconducting wire. Applied Physics Letters. 1986; 48:1403–1405.
21. Chudy M, Zhong Z, Eisterer M, Coombs T. *N*-Values of commercial YBCO tapes before and after irradiation by fast neutrons. Superconductor Science and Technology. 2015; 28:035008.
22. Schild, Th, Maksoud, WA., Aubert, G., Belorgey, J., Bermond, S., Berriaud, C., Bredy, P., Chesny, Ph, Donati, A., Dubois, O., Gilgrass, G., Guillard, JC., Hervieu, B., Juster, FP., Lannou, H., Mayri, C., Meuris, C., Molinié, F., Nunio, F., Quettier, L., Scola, L., Sinanna, A., Tellier, O., Védrine, P. The Iseult/INUMAC whole body 11.7 T MRI magnet R&D program. IEEE Transactions on Applied Superconductivity. 2010; 20:702–705.
23. IEC Standard 60601-2-33. Medical electrical equipment–Particular requirements for the basic safety and essential performance of magnetic resonance equipment for medical diagnosis.
24. Wilson, M. Superconducting Magnets. Vol. Ch.9. Clarendon Pres; Oxford: 1983.
25. Malagoli A, Tropeano M, Cubeda V, Bernini C, Braccini V, Fanciulli C, Romano G, Putti M, Vignolo M, Ferdeghini C. Study of the superconducting and thermal properties of ex-situ glidcop-sheathed practical MgB_2 conductors. IEEE Transactions on Applied Superconductivity. 2009; 19:3670–3674.
26. Brechna, H. Superconducting magnet systems, Vol. 18 of Technische Physik in Einzeldarstellungen. Springer; 1973.
27. Poole, Ch, Baig, T., Deissler, RJ., Doll, D., Tomsic, M., Martens, M. Numerical study on the quench propagation in a 1.5 T MgB2 MRI magnet design with varied wire compositions. Superconductor Science and Technology. 2016; 29:044003.
28. Hahn S, Kim Y, Park DK, Kim K, Voccio JP, Bascuñán J, Iwasa Y. No-insulation multi-width winding technique for high temperature superconducting magnet. Applied Physics Letters. 2013; 103:173511. [PubMed: 24255549]
29. Schild, Th, et al. Towards a new design for a cryogen free MRI magnet. Presentation 4DP1-8, International Magnet Technology Conference MT22; Marseille. September 2011;
30. National Electric Manufacturers Association (NEMA). Publication MW-1000 “Magnet wire”.
31. Yao W, Bascunan J, Kim WS, Hahn, Lee HS, Iwasa Y. A Solid Nitrogen Cooled “Demonstration” Coil for MRI Applications. Superconductor Science and Technology. 2008; 18:912–915.

32. Haid B, Lee H, Iwasa Y, Oh SS, Ha HS, Kwon YK, Ryu KS. Stand-Alone Solid Nitrogen Cooled "Permanent" High-Temperature Superconducting Magnet System. IEEE Transactions on Applied Superconductivity. 2001; 11:2244–2247.
33. Hales PW, Milward S, Harrison S, Jones H. A solid-nitrogen cooled high-temperature Superconducting magnet for use in magneto-hydrodynamic marine propulsion. IEEE Transactions on Applied Superconductivity. 2006; 16:1419–1422.
34. Laskaris ET, Ackermann R, Dorri B, Gross D, Herd K, Minas C. A cryogen-free open superconducting magnet for interventional MRI applications. IEEE Transactions on Applied Superconductivity. 1995; 5:163–168.
35. Tomsic M, Rindfleisch M, Yue J, McFadden K, Phillips J, Sumption MD, Bhatia M, Bohnenstiehl S, Collings EW. Overview of MgB_2 superconductor applications. International Journal of Applied Ceramic Technology. 2007; 4:250–259.
36. Li GZ, Zwayer JB, Kovacs CJ, Susner MA, Sumption MD, Rindfleisch M. Transport critical current densities and n-values of multifilamentary MgB_2 wires at various temperatures and magnetic fields. IEEE Transactions on Applied Superconductivity. 2014; 24(3):6200105.
37. Braccini V, Nardelli D, Penco R, Grasso G. Development of ex situ processed MgB_2 wires and their applications to magnets. Physica C Superconductivity. 2007; 456(1):209–217.
38. Tropeano, M., Grasso, G. MgB_2 development for magnets in medical application. Superconductivity and other new Developments in Gantry Design for Particle Therapy; 17–19 September 2015; see also Columbus Superconductors, http://www.columbussuperconductors.com/mgb2.asp
39. Xu X, Sumption MD, Bhartiya S, Collings EW, Peng X. Critical current densities and microstructures in rod-in-tube and tube type Nb_3Sn strands - Present status and prospects for improvement. Superconductor Science and Technology. 2013; 26(7):075015.
40. Segal C, Tarantini C, Sung ZH, Lee PJ, Sailer B, Thoener M, Schlenga K, Ballarino A, Bottura L, Bordini B, Scheuerlei C, Larbalestier DC. Evaluation of critical current density and residual resistance ratio limits in powder in tube Nb_3Sn conductors. Superconductor Science and Technology. 2016; 29:085003.
41. Motowidlo, L. Method for manufacturing superconductors. US Patent. 7752734. 2010.
42. Miao H, Huang Y, Hong S, Parrell JA. Recent advances in Bi-2212 round wire performance for high field. IEEE Transactions on Applied Superconductivity. 2013; 23(3):6400104.
43. Huang, Y., Miao, H., Hong, S., Gerace, M., Parrell, J. Bi-2212 round wire development and industrialization at OST. WAMHTS-1; Hamburg, Germany. May 21–23, 2014;
44. Ayai N, Kikuchi M, Yamazaki K, Kobayashi S, Yamade S, Ueno E, Fujikami J, Kato T, Hayashi K, Sato K, Hata R, Iihara J, Yamaguchi K, Shimoyama J. The Bi-2223 superconducting wires with 200A-class critical current. IEEE Transactions on Applied Superconductivity. 2007; 17:3075–3078.
45. Breschi M, Casali M, Nayeli N, Corona C, Ribani PL, Trillaud F, Nishijima G. Dependence of Critical Current and Quench Energy of BSCCO-2223 Tapes on Bending Diameter. IEEE Transactions on Applied Superconductivity. 2016; 26:8000605.
46. Zhang Y, Lehner TF, Fukushima T, Sakamoto H, Hazelton DW. Progress in production and performance of second generation (2G) HTS wire for Practical Applications. IEEE Transactions on Applied Superconductivity. 2014; 24(5):7500405. see also Superpower Coil fact sheet http://www.superpower-inc.com/system/files/SP_Coil+Fact+Sheet_2014_v1.pdf.
47. Peng X, Gregory E, Tomsic M, Sumption MD, Ghosh A, Lu XF, Cheggour N, Stauffer TC, Goodrich LF, Splett JD. Strain and magnetization properties of high sub-element count tube-type Nb_3Sn strands. IEEE Transactions on Applied Superconductivity. 2011; 21:2559–2563.
48. Sumption MD, Bhartiya S, Kovacks C, Peng X, Gregory E, Tomsic MJ, Collings EW. Critical current density and stability of tube type Nb_3Sn conductors. Cryogenics. 2012; 52:91–99.
49. Iwasa, Y. Case studies in superconducting magnets. Plenum Press; 1994.
50. Kantorowitz AR, Stekly ZJJ. A new principle for the construction of stabilized superconducting coils. Applied Physics Letters. 1965; 6(56)
51. Yao W, Hahn S, Bascunan J, Iwasa Y. A Superconducting Joint Technique for MgB_2 Round Wires. IEEE Transactions on Applied Superconductivity. 2009; 19:2261–2264. [PubMed: 20671806]

52. Oomen, M., Arndt, T., Haessler, W., Scheiter, J., Ziller, S., Wozniak, M., Hale, H. Superconducting joints between MgB_2 wires for MRI magnets. presentation 2MOr2A-07, Applied Superconductivity Conference; Charlotte, NC. 2014.

53. Patel D, Shahriar M, Hossain A, Maeda M, Shahabuddin M, Yanmaz E, Pradhan S, Tomsic M, Choi S, Kim JH. A new approach to a superconducting joining process for carbon-doped MgB_2 conductor. Superconductor Science and Technology. 2016; 29:095001.

54. Park Y, Lee MW, Oh YK, Lee H. Laser drilling: Enhancing superconducting joint of $GdBa_2Cu_3O_{7-\delta}$ coated conductors. Superconductor Science and Technology. 2014; 27:085008.

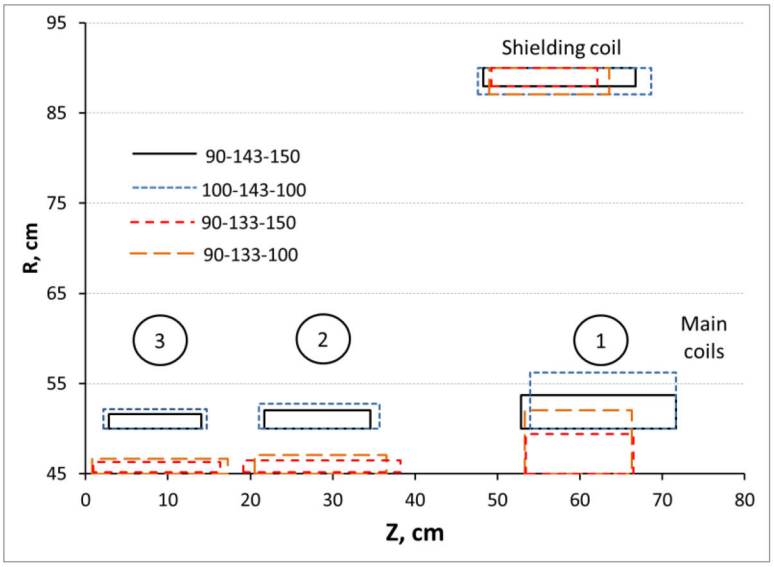

Figure 1.

Coil configurations for MRI magnets

Abbreviation: ID-Length-J_{avg}, where ID is inner diameter of the Main coils (cm), Length is the length of all coils and J_{avg} is the average current density (Amp/mm^2)

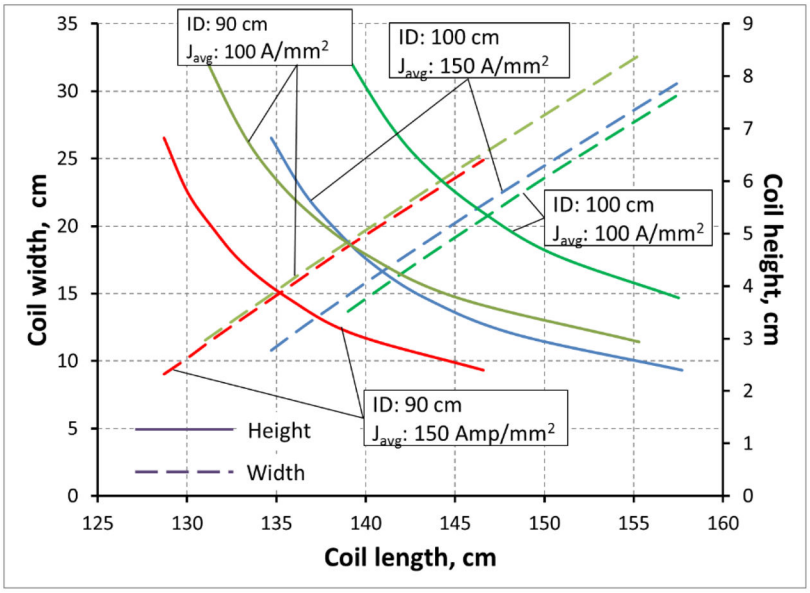

Figure 2.

Width and height of the Main coils #1 vs magnet length, warm bore diameter and current density. “Length” here is specified as the axial distance between superconducting coils. The “length” does not include cryostat.

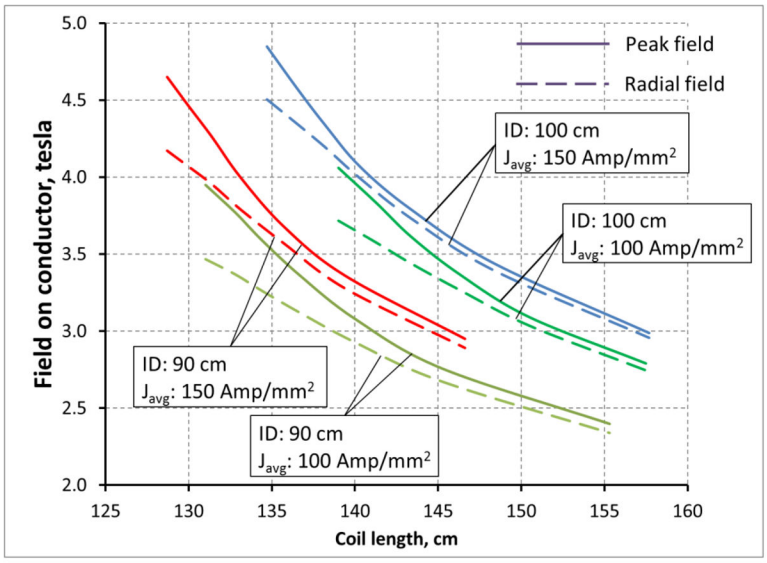

Figure 3.

Peak magnetic field and radial field in the Main coils #1 vs magnet length, bore diameter and current density.

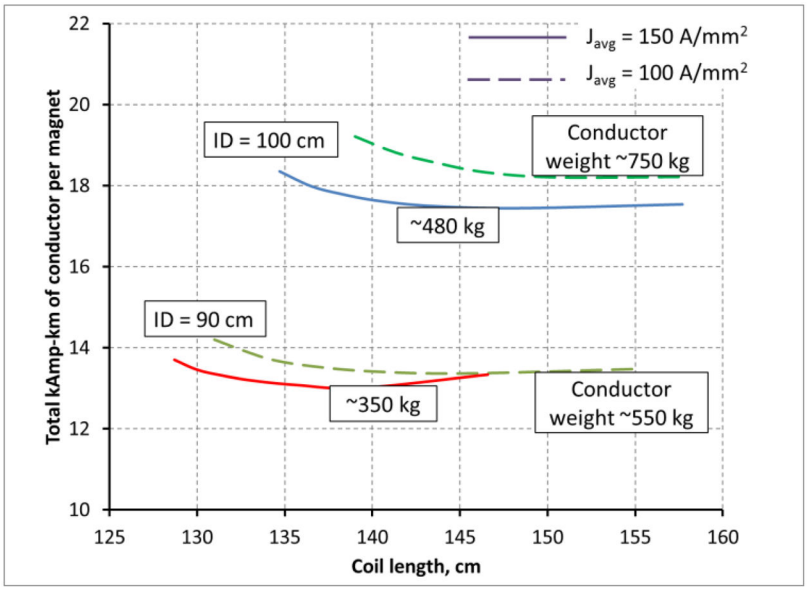

a) Total conductor length

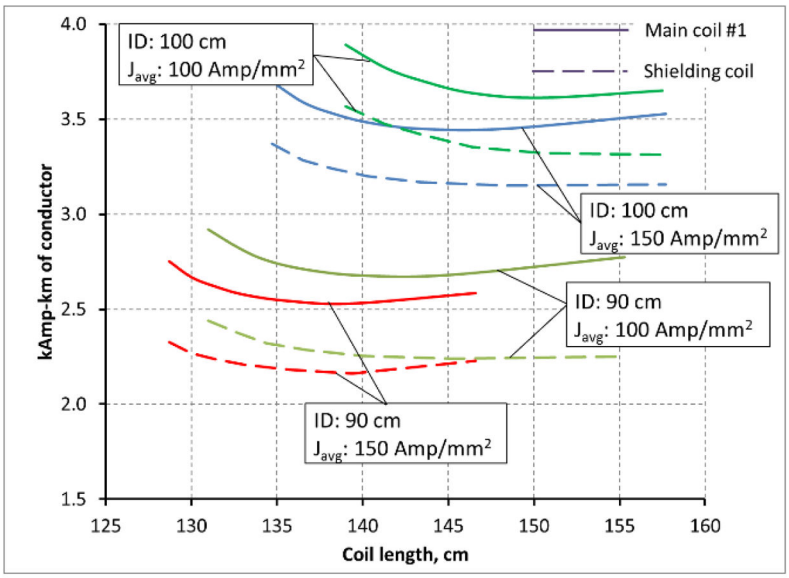

b) Conductor length per coil

Figure 4.
Conductor length requirements

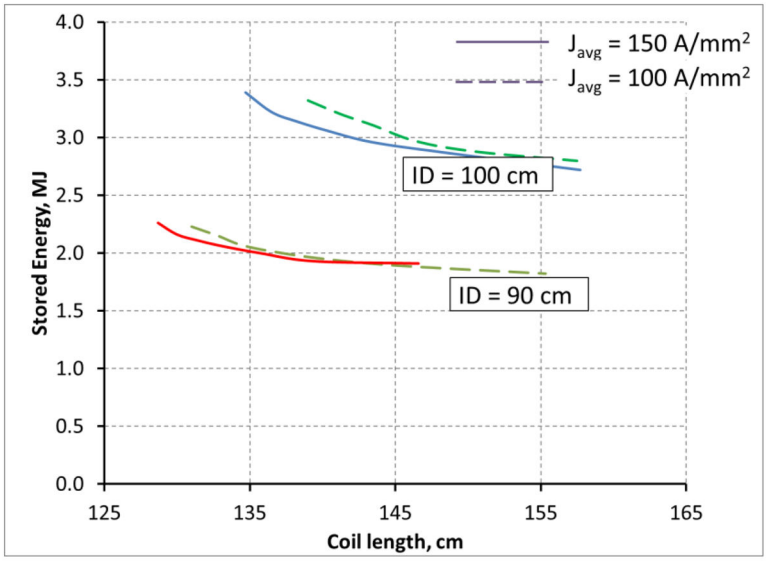

Figure 5.
Stored energy vs length

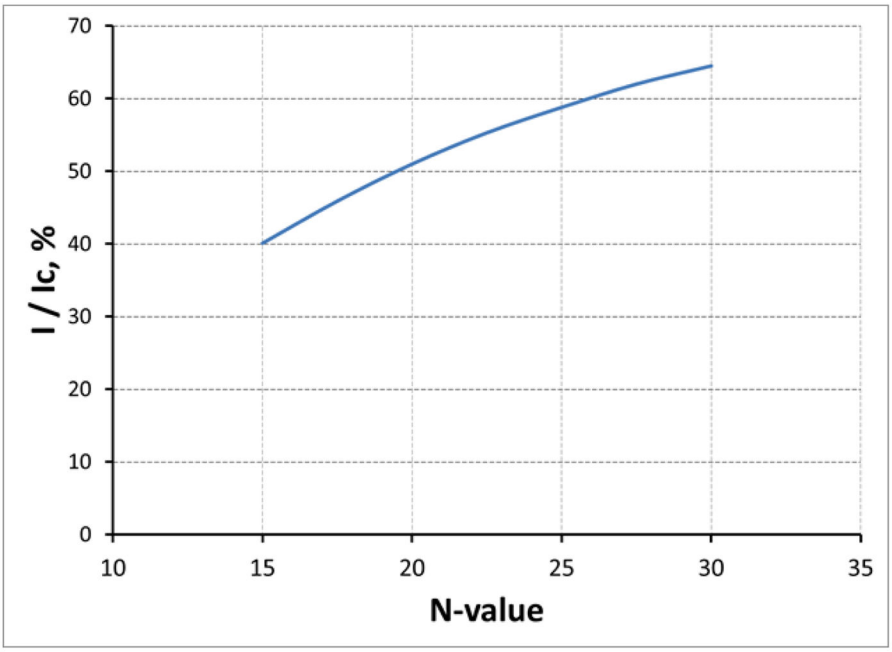

Figure 6.
Operating current vs. ***N***-value

Table 1

Typical parameters of commercial whole-body MRI magnets

	1.5 tesla	3 tesla
Length (including cryostat) *1)*	125 to 170 cm	150 to 180 cm
Patient bore	60 cm (standard bore) and 70 cm (wide bore)	
Warm bore	82 to 93 cm	
Outer diameter (including cryostat)	180 to 210 cm	180 to 210 cm
Design uniformity, 10 ppm peak-to-peak in ellipsoid *2)*	• 30 cm to 45 cm axial direction • 45 cm to 55 cm in radial direction	
Stray field envelope - 5-gauss line (Z × R)	4 m × 2.5 m	5 m × 3 m
Long-term field decay	<0.1% field loss a year	

Notes:

1) In further analysis, we assume that the cryostat length is 20 cm longer than the superconducting coils, and the outer diameter of the cryostat is 20 cm larger than the outer diameter of the coils. Although these lengths depend on the magnet design and cryogenic approach, the values above are within a typical range.

2) The design uniformity in Table 1 assumes fully-shimmed magnet. Shorter magnets may have reduced field of view, especially in the axial direction.

Table 2

1.5 tesla and 3 tesla demonstration smaller-bore HTS magnets

Reference	**[11]**	**[12]**	**[13]**
Organizations	Industrial Research LTD, HTS-110 LTD (New Zealand)	Sumitomo, Kobe Steel, Kyoto University (Japan)	Mitsubishi, Kyoto and Tohoku Universities (Japan)
Application	Ortho	Brain	Animal size demo
Center field, T	1.5	3	2.9
Inner diameter coil, cm	27.6	~60	32
Outer diameter coil, cm	39 estimate[1]	81	42
Length coil, cm	35 estimate	97.2	45
Stored energy, kJ	33 estimate	2,300	250 estimate
Peak field, T	2.2 to 2.5	5.0	4.2
Current, Amp	125	?	185
Average current density, A/mm^2	120 estimate	100 estimate	139
Conductor	YBCO tape	Bi-2223 tape	?
Operating temperature, K	20	20	20
Conductor use, kAmp-km	0.62	8.3	1.8 estimate
Winding type	Double pancakes	Layer-wound, impregnated	Double pancakes
Operating mode	Driven mode	Driven mode 1 ppm/hr @ 1.5T	Driven mode
Uniformity	40 ppm @ 12 cm DSV	5 ppm @ 25×25×20 cm	1.7 ppm @ 10cm VRMS
Stray field (5 gauss, Z × R)	2.7 m × 2.1 m (no yoke)	Unshielded	4.0 m × 3.2 m

[1]"Estimated" parameters in Table 2 are results of reverse engineering carried out by authors of this manuscript. The estimated values were not explicitly provided in the original publications.

Table 3

Design solutions in commercial NbTi-based MRI magnets and potential approaches for MgB_2 / HTS MRI[2]

Areas of design	Present commercial MRI	MgB_2 / HTS MRI
Conductor	* NbTi/Cu, round or rectangular * Graded btw coils and/or layers * Isotropic Ic	* MgB_2 (round); Bi2212 (wire), ReBCO and Bi2223 tapes * Tape graded between pancakes due to Ic anisotropy
Coil topology	* Multicoil design (8 is common) * $\Delta R/\Delta Z \ll 1$ pursued to lower B_{peak}	* Option: axially distributed pancakes; * $\Delta R/\Delta Z > 1$ in pancake design
Coils manufacture & assembly	* Layer winding; epoxy-filled coils * Wound into formers, or in former modules	* React and wind (R&W) or wind-and-react (W&R) * Modular pancakes with ReBCO
Joints	* Superconducting, $R<10^{-11}$ohm each	* Future developments with $R<10^{-11}$ohm, or * Resistive, with high-stability power supply
Formers	* Multi-pocket, or modular assembly * No thermal contact w/coil required	* Require thermal connections in conduction design
Intra-coil stress support	* Axial: through conductor / coil bulk * Hoop: by copper and/or overwrap	* Hoop: reinforcement strip in HTS conductor
Inter-coil force management	* Transfer to formers via flanges or OD/ID	* Axial force transfer through pancakes
Quench protection	* Passive detection; internal protection * Heaters in coils start secondary zones	* Active detection option * External high voltage dump
Current leads	* Insertable, or * Embedded, permanent	* Permanent, to allow external dump
Cooling	* Coils is helium bath; require He vessel * Minimized used helium volume	* Conduction cooling * Convective loops / heat pipes * Higher temp. cryogens, e.g. LH_2 * Thermal battery for ride-through
Shimming	* Passive ferromagnetic shims on trays * Hybrid, with superconducting shim coils	* Passive ferromagnetic shims * Compensation of screening currents
Magnet-gradient interaction	* More pronounced at $B_0 \geq 3$T, with strong gradient coils	* Less sensitive due to higher margin and better accommodation of extra heating

[2]The Nb_3Sn conductor is discussed in Section 5

Table 4

Conductor Requirements for 1.5 T whole-body MRI magnets

Property	Preferred requirements
Conductor shape	Round or rectangular wire (not cable)
Filaments	Multi-filamentary, twisted, <100 mm pitch
Critical current	>500 Amp at 3 tesla and operating temperature
J_{c_eng}, Amp/mm^2	>250 Amp/mm^2 at 3 tesla and operating temperature. J_{c_eng} here includes insulation[4]
N-value	>25 guaranteed over 100% length
Yield strength @ Rp=0.2%	>100 MPa
Bend radius	<50 mm, no I_c degradation
Quench performance	From LN temperature, the conductor shall be able to carry full current for time 10^5 Amp^2_sec/mm^4/ $J_{eng}{}^2$ without overheating above 100°C
Magnetic materials	None (target). If magnetic materials are used, these materials must have predictable and consistent properties over the whole length
Insulation (if used)	Continuous (braid or varnish). Break-down voltage (BDV) > 500 V
Processing	Target: No processing / heat treat after winding
Dimensional tolerances	Less than ±10 micron
Total length, km	20–30 km per magnet
Piece lengths (for layer-wound coils)	70%: more than 3 km Minimum piece length: 1 km

[4] J_{c_eng} is an average (engineering) current density at critical current. J_{eng} is the current density at the nominal current of the magnet.

Table 5

Specifications of alternative conductors for 1.5 T whole-body MRI magnets

Strand	**MgB_2 in-situ**	**MgB_2 ex-situ**	**Bi:2212**	**Bi:2223**	**YBCO**	**Nb_3Sn**
Reference	[35], [36]	[37], [38]	[42], [43]	[44], [45]	[46]	[47], [48]
Selected Manufacturers	HyperTech	Columbus	OST	Sumitomo	Superpower	HyperTech
Shape (R/S/T)[1]	R/RT	R/RT	R	T	T	R
Filament, μm	40	60/400[3]	200	200	4000	30
Twist, mm	20	300	80	3–8	none	20
Standard bare diameter or cross-section dimensions	1.2[2]	3 × 0.5	1.2	4.3 × 0.23	4.0 × 0.1	0.5
I_c, @ std dia (4K, 3.5 T)	500 *note 4*	300	600	520	400	650
$J_{e,w}$ (4K, 3.5 T)[5] A/mm[2]	385	125	530	425	850 (⊥)	2870
Yield Strength, MPa	200	120	120–150	130	550	
Min Bend R, mm (W&R) R&W[6]	(16) 150	62.5 (easy)	100	80	11 (easy)	(10) 62.5
Protection time, sec (with added stabilizer to reach 250 A/mm[2])	Very small (2.4 sec)	--	0.35 (3.2)	0.55 (2.7)	0.13 (5.5)	0.012 (18)
Magnetic materials used?	Yes, 100 mT	Yes	None	None	None	None
Wind-and-react (W&R), React-and-wind (R&W)	R&W W&R	NA	W&R	R&W	NA	W&R R&W
Piece length, km	3	>1	1	1.5	1	2
N-value	30	20–40	15–20	15–20	> 25	>30
Persistent joints?	Y	Y	N	N	N	Y

Notes

[1] Round (R), rectangular (RT), or Tape (T)

[2] While not presently commercial, minimal development needed

[3] Anisotropic, both values given

[4] Based on J_C of 3×10^5 A/cm^2 at 4 K, 3.5 T, a fill factor of 15%

[5] Based on 15 % for insulation, except NbTi, for which no reduction was taken

[6] Bi:2212 strain 0.6%. Using strain = $t/2R$, or $R=OD/2$(strain) For Nb_3Sn, 0.4% for MgB_2, 0.4%, and 0.2% for Bi:2223